Molecular Systems Biology 4; Article number 219; doi:10.1038/msb.2008.56
Citation: ***Molecular Systems Biology*** **4:219**

www.molecularsystemsbiology.com

molecular systems biology

Systemic multicompartmental effects of the gut microbiome on mouse metabolic phenotypes

Sandrine P Claus[1], Tsz M Tsang[1], Yulan Wang[2], Olivier Cloarec[1], Eleni Skordi[1], François-Pierre Martin[3], Serge Rezzi[3], Alastair Ross[3], Sunil Kochhar[3], Elaine Holmes[1] and Jeremy K Nicholson[1,*]

[1] SORA Division, Department of Biomolecular Medicine, Imperial College London, London, UK, [2] State Key Laboratory of Magnetic Resonance and Atomic and Molecular Physics, Wuhan Centre for Magnetic Resonance, Wuhan Institute of Physics and Mathematics, The Chinese Academy of Sciences, Wuhan, PR China and [3] BioAnalytical Science Department, Nestlé Research Center, Lausanne, Switzerland
* Corresponding author. SORA Division, Department of Biomolecular Medicine, Imperial College London, Sir Alexander Fleming Building, South Kensington, London SW7 2AZ, UK. Tel.: +44 (0)207 594 3195; Fax: +44 (0)207 594 3221; E-mail: j.nicholson@imperial.ac.uk

Received 24.4.08; revised 15.7.08

To characterize the impact of gut microbiota on host metabolism, we investigated the multicompartmental metabolic profiles of a conventional mouse strain (C3H/HeJ) (n=5) and its germ-free (GF) equivalent (n=5). We confirm that the microbiome strongly impacts on the metabolism of bile acids through the enterohepatic cycle and gut metabolism (higher levels of phosphocholine and glycine in GF liver and marked higher levels of bile acids in three gut compartments). Furthermore we demonstrate that (1) well-defined metabolic differences exist in all examined compartments between the metabotypes of GF and conventional mice: bacterial co-metabolic products such as hippurate (urine) and 5-aminovalerate (colon epithelium) were found at reduced concentrations, whereas raffinose was only detected in GF colonic profiles. (2) The microbiome also influences kidney homeostasis with elevated levels of key cell volume regulators (betaine, choline, *myo*-inositol and so on) observed in GF kidneys. (3) Gut microbiota modulate metabotype expression at both local (gut) and global (biofluids, kidney, liver) system levels and hence influence the responses to a variety of dietary modulation and drug exposures relevant to personalized health-care investigations.
Molecular Systems Biology 14 October 2008; doi:10.1038/msb.2008.56
Subject Categories: metabolic and regulatory networks; microbiology and pathogens
Keywords: germ-free; gut microbiota; metabolism; metabonomics

Introduction

The gut microbiota (microbiome) form a complex and dynamic ecosystem that constantly interacts with host metabolism (Dunne, 2001; Hooper and Gordon, 2001; Bourlioux *et al*, 2003). The microbiome provides trophic (Hooper and Gordon, 2001) and protective (Umesaki and Setoyama, 2000) functions and impact on the host's energy metabolism (Savage, 1986), facilitating the absorption of complex carbohydrates (fiber breakdown) and influencing the homeostasis of amino acids (Hooper *et al*, 2002). For example in humans, 1–20% of the circulating plasma lysine and threonine are derived from gut bacterial synthesis (Metges, 2000). The microbiota also synthesize essential vitamins such as vitamin K (Hooper *et al*, 2002) and group B vitamins (Burkholder and McVeigh, 1942). These close symbiotic relationships are the result of co-evolutionary processes, through which natural selection has promoted the host genotypes that provide well-adapted adhesion sites for specific microorganisms (Bäckhed *et al*, 2005). In total, the mammalian symbiotic superorganism can contain significantly more active DNA in the fan of genes from the microbiome than in the host genome (Nicholson *et al*, 2005). Indeed, the symbiotic microbiotal speciation of some invertebrates (e.g. plataspid insects) has been shown to be closely connected with host evolution and take control of many metabolic functions resulting in host genome reduction (Hosokawa *et al*, 2006). The indigenous microbiota of mammals also strongly influences the metabolism of many drugs and nutrients, modifying both their bioavailability and metabolic fate (Nicholson *et al*, 2005). For example, phytoestrogens are metabolized into active compounds by gut microbiota (Setchell, 1998; Atkinson *et al*, 2005). But despite their evident important contribution to host biology and function, some bacterial species contained in the gut also have the potential to generate carcinogens or can be the source of opportunistic infections (Berg, 1996). For instance,

Helicobacter pylori is well known to be part of the commensal flora of the stomach that can cause gastritis, gastric ulcers and, in some cases, gastric cancer (Amieva and El-Omar, 2008).

We have recently demonstrated a close relationship between the metabolism of gut microbiota and the susceptibility of rodents to insulin resistance in high-fat diet studies (Dumas *et al*, 2006a). In this context, recent works have shown that even subtle changes in the gut microbiota have an impact on the host phenotype (Holmes and Nicholson, 2005; Robosky *et al*, 2005; Rohde *et al*, 2007). Other investigations have demonstrated the close link between obesity and gut microbiota in human and mice (Bäckhed *et al*, 2004, 2007; Ley *et al*, 2006; Turnbaugh *et al*, 2006).

Germ-free (GF) animal studies have been widely used as a source of knowledge on the gut microbiota contributions to host homeostatic controls (Wostmann, 1981). GF mice display unusual gut morphology, i.e. larger cecum, thinner intestinal villi, when compared with conventional animals as well as physiological and immunological abnormalities, i.e. lower peristalsis, decreased inflammatory responses (Berg, 1996). GF animals have also been used to observe the developmental mechanisms of the gastrointestinal tract in interaction with the gut microbiota (Bates *et al*, 2006). However, despite the extensive use of GF models, the exact mechanisms involved in the morphologic, physiologic and immunologic modifications in GF animals remain unclear. The characterization of the metabolic differences between conventional and GF mice is, therefore, an essential step toward better understanding the interaction between host and gut microbiota.

Metabonomic approaches combining spectroscopic profiling techniques with pattern recognition analysis have proved useful in the assessment of the systemic metabolic responses of organisms to drugs or nutrients (Nicholson *et al*, 2002; Lindon *et al*, 2004; Dumas *et al*, 2006b; Rezzi *et al*, 2007). This approach has been successfully applied on biofluids and intact intestinal tissues in rodents to demonstrate the involvement of microbiota in the mammalian metabolism (Nicholls *et al*, 2003; Wang *et al*, 2005; Martin *et al*, 2006). In addition, metabonomic approaches have been recently used to demonstrate that hippurate excretion, a marker of gut microbiotal activity in protein catabolism to benzoate, varies between normal and obese rats (Williams *et al*, 2005) and the close link between gut microbiota and fatty liver phenotype in insulin-resistant mice (Dumas *et al*, 2006a).

In the current study, we employed a high-resolution ^{1}H NMR spectroscopic approach to investigate the metabolic phenotype, or metabotype (Gavaghan *et al*, 2000), of GF mice from urine and tissues (gut, liver and kidney) and to determine the biochemical consequences of the absent microbiome on these biological matrices.

Results

Spectra from biofluids and tissue aqueous extracts contain prominent signals from metabolites representing numerous major metabolic pathways. For each analyzed biological matrix, a typical spectrum obtained from a conventional and a GF mouse is displayed (Figures 1A and B, 2A and B, 3A and B, 4A and B, and 5A and B) and Table I shows the NMR assignment and corresponding resonance multiplicity. The summaries of all statistical models are shown in Table II. The main metabolic differences in GF group were summarized for all biological matrices in Table III.

Urine

The urine profile was characterized by high levels of taurine, 2-oxoglutarate, trimethylamine (TMA), citrate and succinate as previously reported (Bollard *et al*, 2005) (Figure 1A and B). The urinary profile of GF mice was characterized by low levels of hippurate, phenylacetylglycine (PAG), phenolic metabolites, 4-hydroxypropionic acid (4-HPP), 3-hydroxycinnamic acid (3-HCA) and *N*-acetylated glycoprotein signal and a marked high level of creatinine (Figure 1C).

Liver

Glucose resonances (δ 3.25–3.84) were predominant in the liver profile, which was also dominated by high levels of taurine and trimethylamine-*N*-oxide (TMAO) (Figure 2A and B). The oxidized glutathione (GSSG) pattern was readily identified in the one-dimensional (1D) spectrum. It is possible to differentiate between the reduced (GSH) and the oxidized (GSSG) forms of glutathione by 2D NMR because the resonances of the magnetically non-equivalent protons of the cysteine β-CH_2 residue in GSH (δ 2.95) shift to high frequency in GSSG (δ 3.29 and 2.95) (Koga *et al*, 1986). The statistical model built from all liver spectra displayed an outlier in the GF group (data not shown). This highly dilute sample was removed from the subsequent analysis and the model was recalculated with four individuals in the GF group against five individuals in the conventional group. The metabolite profile of the liver from GF mice exhibited significant higher levels of TMAO and phosphocholine. Not significant higher levels of tauro-conjugated bile acids and glycine were noted in the GF mouse profile (Figure 2C). In addition, a lower level of GSSG together with a higher level of hypotaurine was observed in the liver of two GF animals.

Kidney

The kidney ^{1}H NMR profiles were dominated by osmoprotectant compounds such as *myo*-inositol, glycine, betaine, choline and taurine (Yancey, 2005) (Figure 3A and B). The metabolite profile of the kidney from GF mice was characterized by higher levels of betaine, choline, *myo*-inositol, *scyllo*-inositol, ethanolamine, inosine and an unknown compound (U1) in the aromatic region of the spectra (δ 7.14 (d) and δ 7.30 (d)) (Figure 3C).

Gut compartments

Duodenum, jejunum and ileum were all characterized by high levels of tyrosine when compared with the other tissue extracts (Figure 4A, B; Supplementary Figures S1A and B, and S2A and B) together with creatine and taurine, a feature shared with the colon (Figure 5A and B). The colonic metabolite profile was characterized by high levels of *myo*-inositol and *scyllo*-inositol,

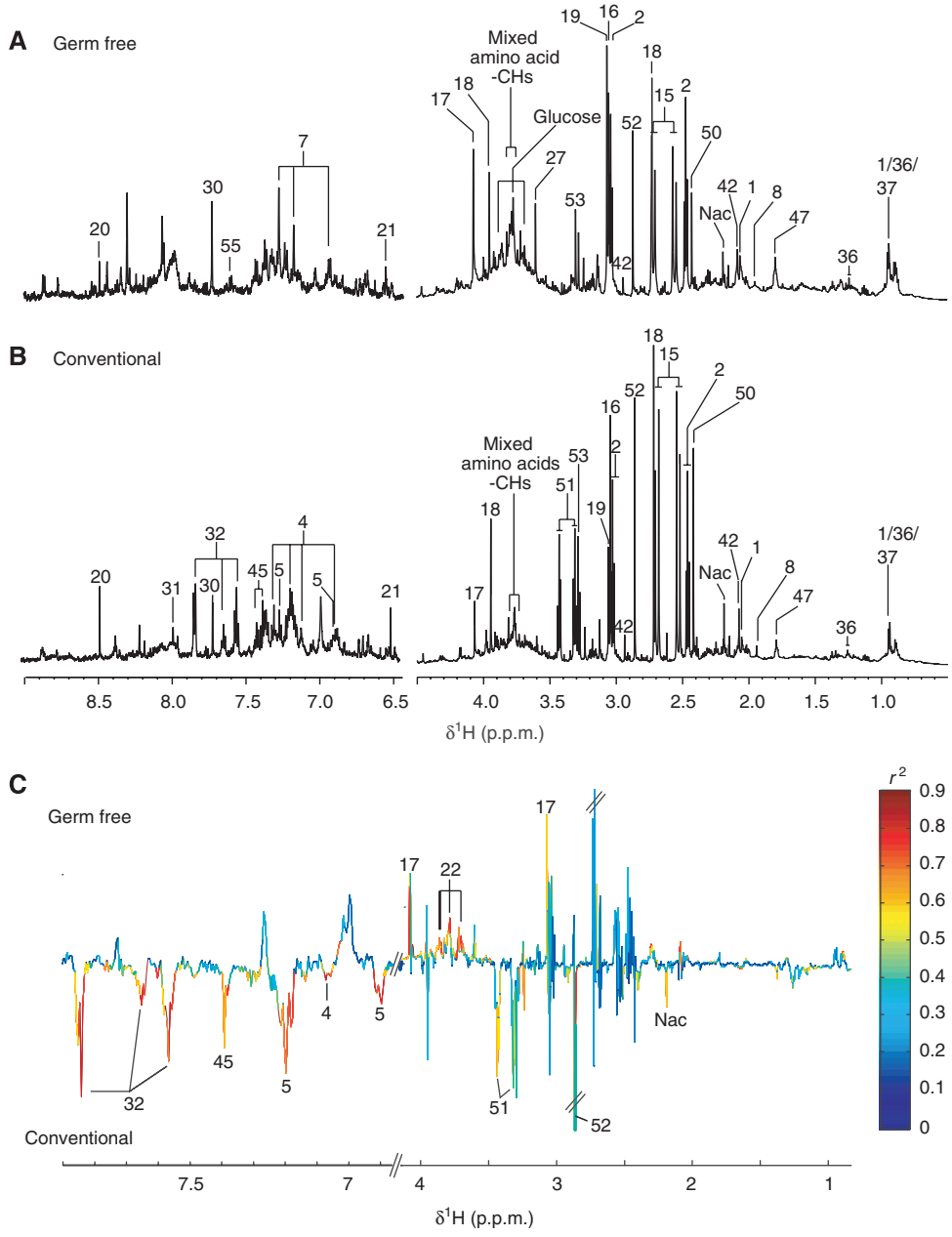

Figure 1 ^{1}H NMR spectra (600 MHz) of urine samples from germ-free (GF) (**A**) and conventional (**B**) mice. The aromatic region (δ 6.5–9.0) has been vertically expanded × 4. (**C**) Plot of O-PLS-DA coefficients related to the discrimination between ^{1}H NMR spectra of urine from GF (top) and conventional (bottom) mice. For identification of the peak numbers, refer to codes in Table II.

as previously described (Martin *et al*, 2007b) (Figure 5A). Globally, these gut profiles also displayed similar patterns to those observed in human biopsies (Wang *et al*, 2007). Tauro-conjugated bile acids were observed only in duodenum, ileum and jejunum profiles.

Aqueous extract profiles of gut tissues from GF mice were markedly different to those from conventional mice (Figures 4C and 5C; Supplementary Figures S1C and S2C). The metabolite profile of the duodenum from GF mice was mainly characterized by higher levels of tauro-conjugated bile acids and alanine and lower levels of glycerophosphocholine (GPC) when compared with conventional mice (Supplementary Figure S1C). Two highly diluted samples in the jejunum profiles of the GF group were outliers and hence orthogonal projection on latent structures (O-PLS-DA) correlation coefficients (r^2) were not significant (Supplementary Figure S2C). However, the GF group had higher levels of creatine and tauro-conjugated bile acids and lower levels of tyrosine in the jejunal tissue (Supplementary Figure S2C). The ileum of GF mice was also characterized by a higher level of tauro-conjugated bile acids and lower levels of glutamate, fumarate, lactate, phosphocholine and alanine when compared with the ileum from conventional mice (Figure 4C). Finally, when compared with conventional mice, the metabolite profile of the colon

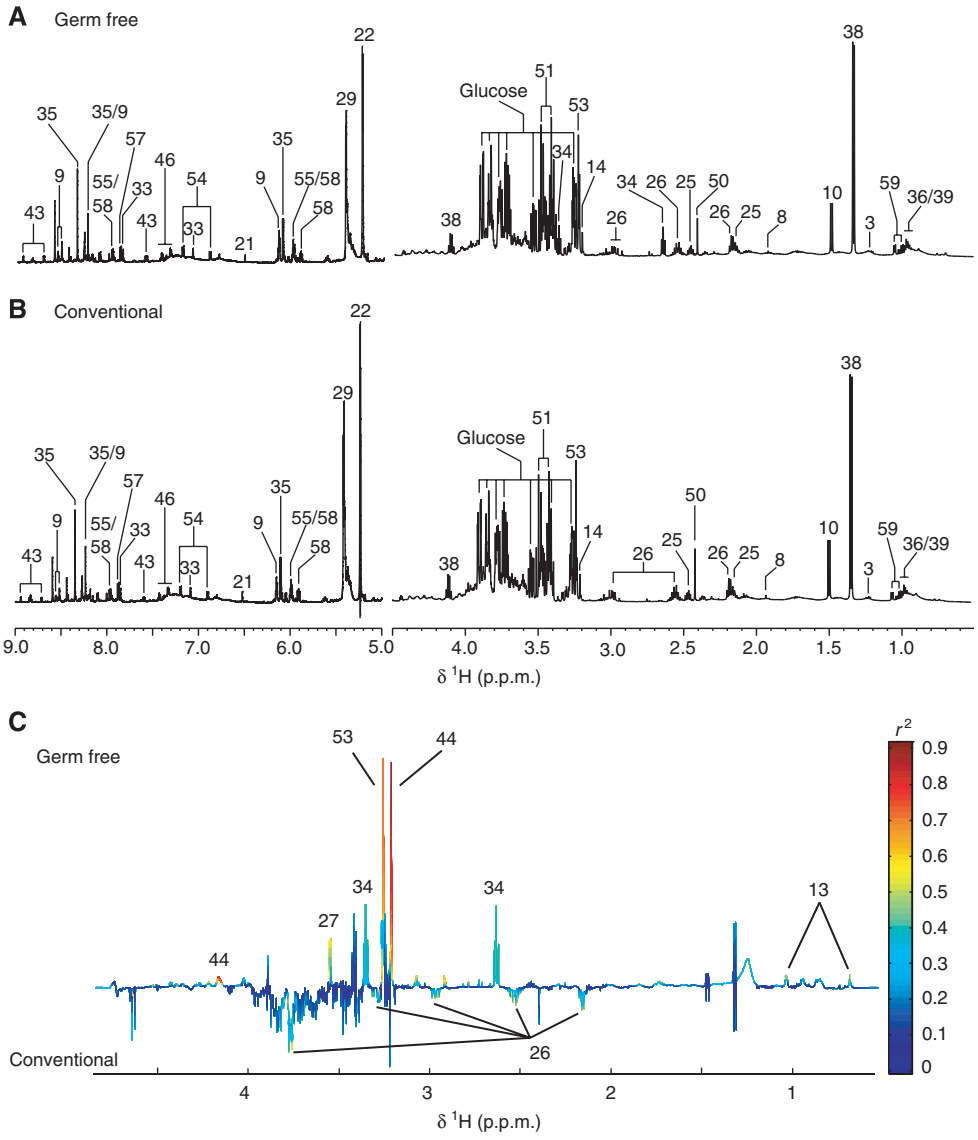

Figure 2 ^{1}H NMR spectra (600 MHz) of liver aqueous extracts of germ-free (GF) (**A**) and conventional (**B**) mice. The aromatic region (δ 6.5–9.0) has been vertically expanded ×4. (**C**) Plot of O-PLS-DA coefficients related to the discrimination between ^{1}H NMR spectra of urine from GF (top) and conventional (bottom) mice. For identification of the peak numbers, refer to codes in Table II.

from GF mice revealed a higher level in a complex carbohydrate identified as raffinose (Supplementary Figure S3), and lower levels of lactate, creatine, 5-aminovalerate, propionate, glutamine, *myo*-inositol, *scyllo*-inositol (Moreno and Arus, 1996), GPC, phosphocholine, choline, formate, uracil and fumarate (Figure 5C).

Discussion

In this study, the metabotypes derived from different biological matrices from GF and conventional mice were characterized (Nicholson *et al*, 2002; Lindon *et al*, 2004) and it was showed that the metabolic impact of the microbiota extended beyond the intestinal tissue and biofluids to major organs such as the liver and kidney.

Evidence of gut microbiota re-processing of dietary metabolites

A major source of the intestinal metabolites is produced from dietary nutrients by both the intestinal cells and the gut microbiota. This production occurs mainly in the first 25% of the small intestine for amino acids, and in cecum and colon for fatty acids (Hooper *et al*, 2002). Here, metabolic variations in response to gut microbial activity are observed in the biochemical profiles of intestinal tissue extracts with increasing effect along the continuous gastrointestinal tract. More specifically, it was observed that duodenum and jejunum displayed fewer metabolic differences between GF and conventional mice, whereas ileum and particularly colon were the most affected (Table III). This reflects the higher microbial loads found in ileum and colon (Dunne, 2001). In particular,

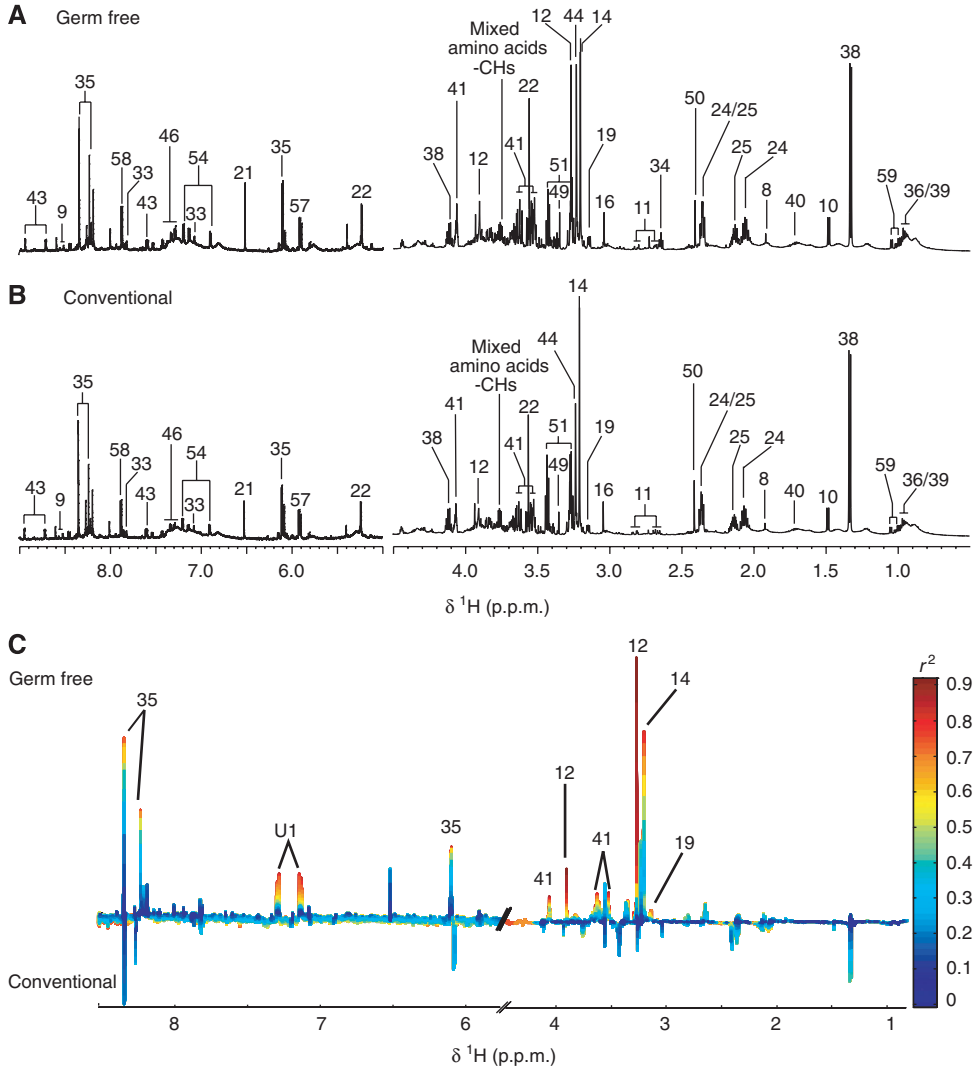

Figure 3 ^{1}H NMR spectra (600 MHz) of kidney aqueous extracts of germ-free (GF) (**A**) and conventional (**B**) mice. The aromatic region (δ 6.5–9.0) has been vertically expanded × 4. (**C**) Plot of O-PLS-DA coefficients related to the discrimination between ^{1}H NMR spectra of urine from GF (top) and conventional (bottom) mice. For identification of the peak numbers, refer to codes in Table II.

5-aminovalerate was not observed in colon aqueous extract profiles of GF animals, which is consistent with its reported characterization as a product of protein degradation by several anaerobic bacteria, particularly clostridial strains (Figure 5C) (Barker, 1981; Barker *et al*, 1987). 5-Aminovalerate is degraded to acetate, ammonia and propionate. A higher concentration of propionate also observed in colon profile of conventional mice is consistent with the higher concentration of 5-aminovalerate.

More evidence of the crucial role of gut bacteria in the digestion of dietary nutrients is seen in the lower urinary level of several microbial co-metabolites (hippurate, 4-HPP and 3-HCA) in GF mice (Figure 1C). Indeed, it has been reported that gut microbiota are able to metabolize polyphenols, such as chlorogenic acids, into more absorbable compounds such as 4-HPP, 3-HCA and benzoic acid (Goodwin *et al*, 1994; Manach *et al*, 2004). Benzoic acid is then detoxified through conjugation with glycine in the liver and the kidney to form hippurate (benzoylglycine), a more hydrophilic metabolite that is then secreted by the renal tubular cells and excreted in the urine (Goodwin *et al*, 1994; Williams *et al*, 2002; Nicholls *et al*, 2003). Another microbial co-metabolite, PAG, was also found in lower concentration in the urinary profile of GF animals (Figure 1C), illustrating that microorganisms are crucial actors in the production of these urinary metabolites through the modulation of food processing.

Evidence of the host–gut bacterial metabolic interaction: bile acid co-metabolism

The metabolism and synthesis of the major bile acids are another example of mammalian–microbiotal co-metabolism that has been reported recently as crucial in determining the host phenotype (Martin *et al*, 2007a). In the present study, the metabolite profiles of duodenum, jejunum and ileum (Figure 4C) were all characterized by a higher concentration of tauro-conjugated bile acids in GF mice, which is not apparent in the colon profile (Figure 5C). In conventional animals, tauro- and glycine-conjugated bile acids are deconjugated by

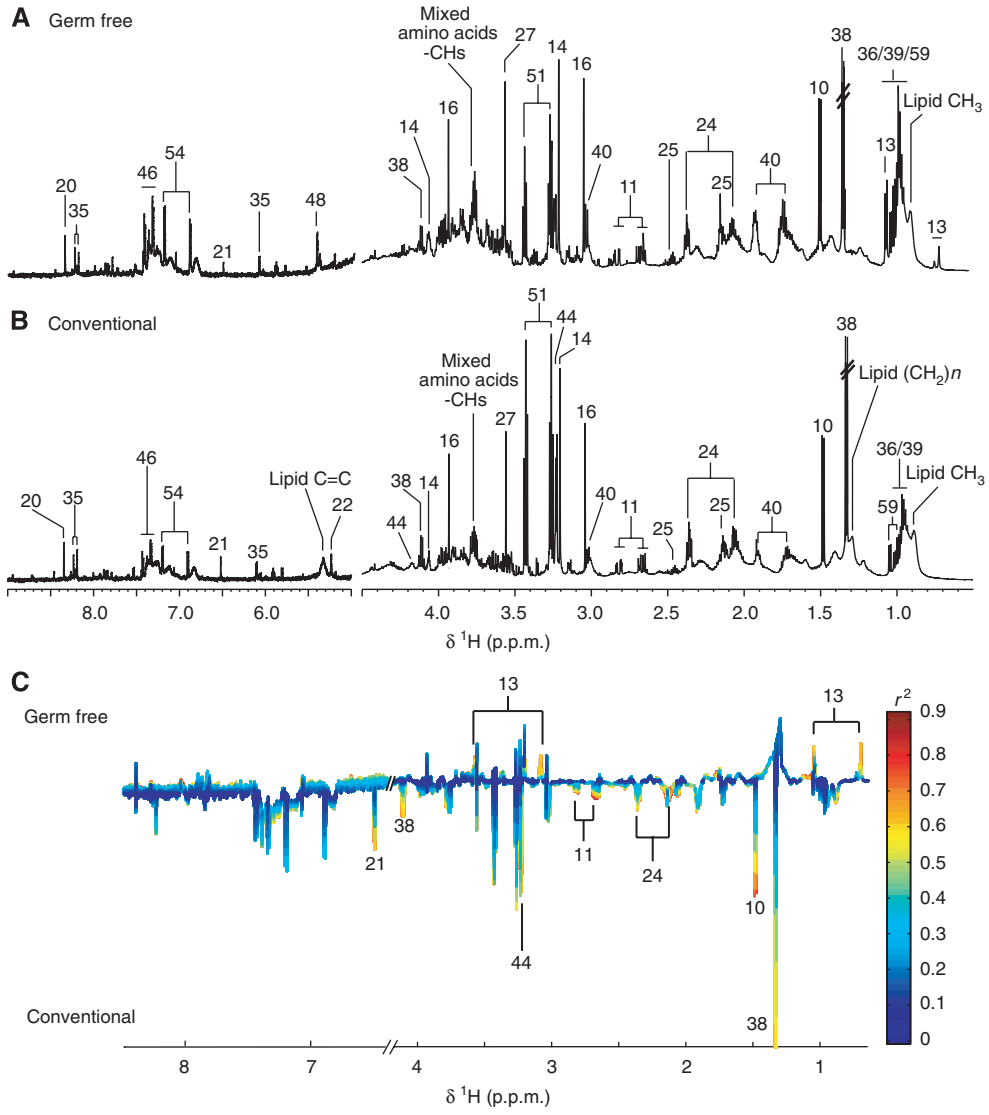

Figure 4 ^{1}H NMR spectra (600 MHz) of ileum aqueous extracts of germ-free (GF) (**A**) and conventional (**B**) mice. The aromatic region (δ 6.5–9.0) has been vertically expanded ×4. (**C**) Plot of O-PLS-DA coefficients related to the discrimination between ^{1}H NMR spectra of urine from GF (top) and conventional (bottom) mice. For identification of the peak numbers, refer to codes in Table II.

gut microbiota, facilitating their fecal elimination. Here, in the absence of microorganisms, primary bile acids are reabsorbed into the enterohepatic cycle, without deconjugation, by passive diffusion in duodenum and jejunum and by active transport in the terminal part of the ileum (Berg, 1996; Houten *et al*, 2006) (Figure 7). This increased recycling of bile acids is also suggested by the significantly higher level of phosphocholine and by the observed trend of higher concentration of bile acids in the liver metabolic profile of GF mice (Figure 2C). In fact, phosphocholine is the source of phosphatidylcholine, the most common phospholipid in bile, and its secretion is under control of certain bile acids, mainly cholic acid and deoxycholic acid, in hepatocytes (Uchida *et al*, 1980; Alvaro *et al*, 1986; Hofmann, 1999). Thus, the observation of the higher level of phosphocholine in liver GF profile may be the result of either a modification of bile acid profile or a higher level of bile acids in hepatocytes.

Microbial modification of bile acid metabolism may have many biological consequences, as bile acids participate in the regulation of dietary lipid absorption and cholesterol metabolism. They also function as signaling molecules linking to a G-protein-coupled receptor family (Kawamata *et al*, 2003; Kostenis, 2004) or directly triggering the farnesoid X receptor (FXR), which is a hepatocyte nuclear receptor involved in the regulation of lipid and glucose metabolism (Makishima *et al*, 1999; Claudel *et al*, 2005; Modica and Moschetta, 2006). Bile acids exert strong influences on the regulation of the expression of some cytochrome *P*450 (CYP) detoxification enzymes in the liver (Houten *et al*, 2006). It is also well known that CYP are key enzymes in the production of bile acids from cholesterol (Russell, 2003). Furthermore, Gram-negative bacteria produce endotoxins (lipopolysaccharides) that affect the expression of some CYP enzymes in the liver (Ueyama *et al*, 2005). Thereby, the microbiota may have an impact on

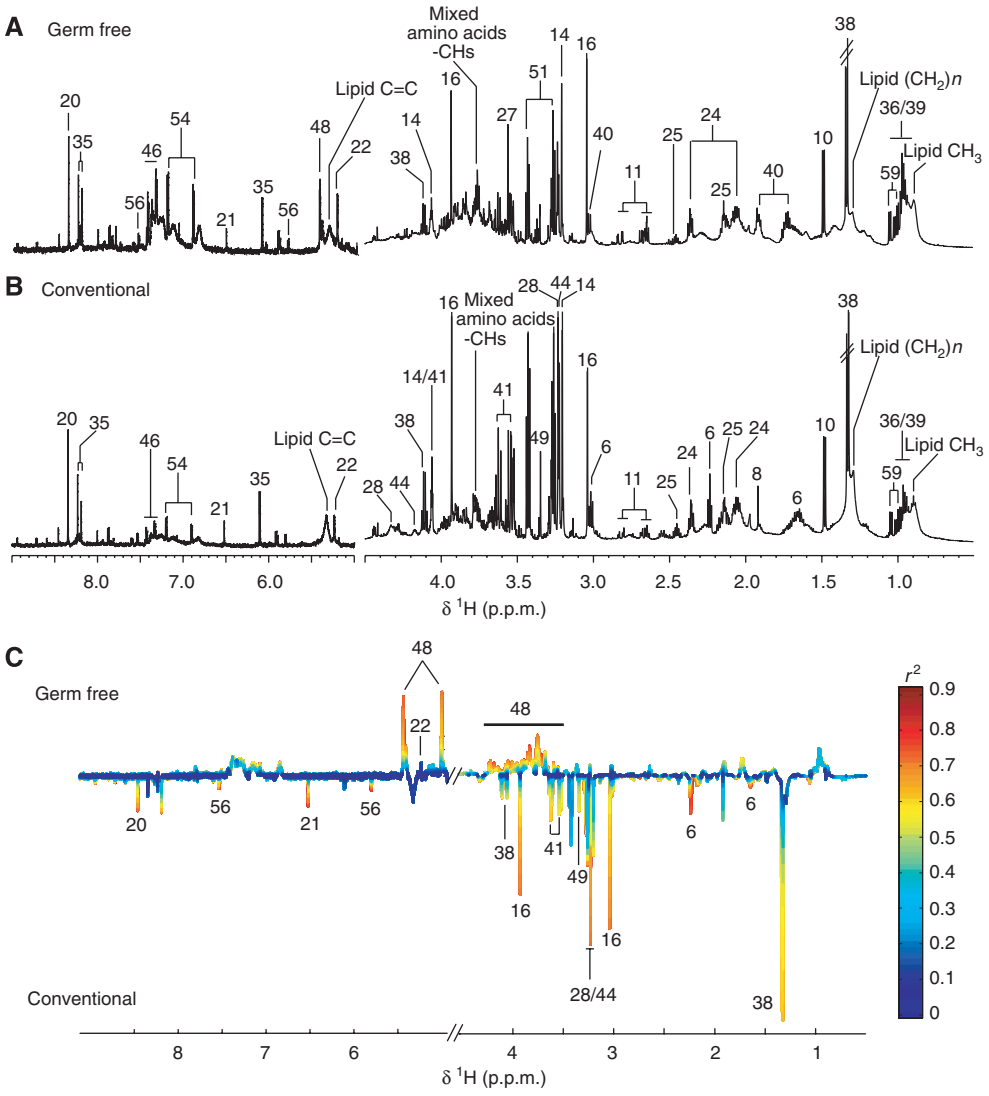

Figure 5 ^{1}H NMR spectra (600 MHz) of colon aqueous extracts of germ-free (GF) (**A**) and conventional (**B**) mice. The aromatic region (δ 6.5–9.0) has been vertically expanded × 4. (**C**) Plot of O-PLS-DA coefficients related to the discrimination between ^{1}H NMR spectra of urine from GF (top) and conventional (bottom) mice. For identification of the peak numbers, refer to codes in Table II.

host energy homeostasis by participating, directly or indirectly, in the control of bile acid metabolism.

Evidence of the modulation of host cell pathways and physiology by gut microbiota

The colonic metabolite profile in GF mice was characterized by lower levels of choline and its phosphorylated derivatives, GPC and phosphocholine. This is likely due to the disturbance of the membrane of colonocytes in GF animals. The observed accumulation of raffinose in these cells is probably also a consequence of this disruption. Raffinose is an oligosaccharide that is only digested by the gut microbiota, as monogastric animals do not express pancreatic α-galactosidase (LeBlanc *et al*, 2004). In GF animals, it seems that this trisaccharide is able to cross the epithelial membrane and accumulates in colonocytes where it induces a rise in osmotic pressure. This phenomenon provokes a well-described signaling cascade that leads to the release of the mobile osmolytes, GPC, *myo*-inositol and *scyllo*-inositol (Wehner, 2003; Alfieri, 2007) (Figure 6). Interestingly, lower levels of these metabolites have previously been associated with human colon adenocarcinoma (Moreno and Arus, 1996), and have also been observed in the brain of patients with hepatic encephalopathy (Lien *et al*, 1994; Albrecht and Jones, 1999) or associated with osmoregulatory function in the brain in response to atrophy (Tsang *et al*, 2006). These physiological changes were correlated with significantly lower creatine concentrations that can be associated with lower energy demands and with a lower peristalsis due to an impaired function of the smooth muscle layer in GF mice (Berg, 1996). Furthermore, a number of metabolites involved directly (e.g. fumarate) or indirectly (e.g. glutamate, aspartate, alanine and lactate) in energy pathways were present at lower levels in the ilial and colonic epithelium. Aspartate and fumarate are also key metabolites in the metabolism of urea associated with the citric acid cycle, a pathway that enables the

Table I Full ^{1}H NMR chemical shift data for discriminating metabolites assigned in urine and tissue samples (note that signals for unassigned or non-significantly discriminating metabolites are not reported)

Code	Metabolite	δ ^{1}H (multiplicity) group	Compartments observed
1	2-Oxoisocaproate	0.94 (d) CH_3, 2.18 (m) CH, 2.64 (d) CH_2	U
2	2-Oxoglutarate	2.47 (t) γCH_2, 3.03 (t) βCH_2	U
3	D-3-Hydroxybutyrate	1.20 (d) CH_3, 2.31 (dd) $\frac{1}{2}$ αCH_2, 2.41 (dd) $\frac{1}{2}$ αCH_2, 4.16 (dt) CH	L
4	3-Hydroxycinnamate	6.49 (d) αCH, 6.92 (d) H2, 7.09 (s) H6, 7.17 (d) H4, 7.33 (m) H3/β-CH	U
5	4-Hydroxyphenylpropionate	2.52 (t) αCH, 2.91 (t) βCH, 6.92 (d) H2/H6, 7.22 (d) H3/H5	U
6	5-Aminovalerate	1.64 (m) $\beta/\gamma CH_2$, 2.25 (t) αCH_2, 3.02 (t) δCH_2	C
7	5-Hydroxytryptophan	3.23 (dd) $\frac{1}{2}$ βCH_2, 3.41 (dd) $\frac{1}{2}$ βCH_2, 4.02 $CHNH_2$, 6.88 H6, 7.14 H2, 7.28, 7.41 H7	U
8	Acetate	1.92 (s) CH_3	U, L, K, D, J, I, C
9	Adenosine diphosphate	4.20 (dd) $\frac{1}{2}$ CH_2, 4.23 (dd) $\frac{1}{2}$ CH_2, 4.27 (dt) H5, 4.50 (m) H4, 4.77 (m) H3, 6.12 (d) H2, 8.18 (s) H7, 8.50 (s) H12, 8.55 (s) H12	L, K
10	Alanine	1.48 (d) βCH_3, 3.79 (m) CH	L, K, D, J, I, C
11	Aspartate	2.68 (AB of ABX) $\frac{1}{2}$ βCH_2, 2.82 (AB of ABX) $\frac{1}{2}$ βCH_2, 3.91 (X of ABX) αCH	K, D, J, I, C
12	Betaine	3.27 (s) CH_3, 3.90 (s) CH_2	K
13	Bile acids (mixed)	0.70 (s) CH_3, 1.05 (s) CH_3	L, D, J, I
14	Choline	3.20 (s) N-$(CH_3)_3$, 3.51 (t) βCH_2, 4.05 (t) αCH_2	L, K, D; J, I, C
15	Citrate	2.69 (AB) $\frac{1}{2}$ CH_2, 2.55 (AB) $\frac{1}{2}$ CH_2	U
16	Creatine	3.03 (s) N-CH_3, 3.94 (s) CH_2	U, K, D, J, I, C
17	Creatinine	3.06 (s) N-CH_3, 4.05 (s) CH_2	U
18	Dimethylamine	2.72 (s) CH_3	U
19	Ethanolamine	3.13 (t) NH-CH_2, 3.83 (t) HO-CH_2	K
20	Formate	8.46 (s) CH	U, D, J, I, C
21	Fumarate	6.52 (s) CH	U, L, K, D, J, I, C
22	α-Glucose	3.42 (t) H4, 3.54 (dd) H2, 3.71 (t) H3, 3.72 (m) $\frac{1}{2}$ CH_2-C6, 3.76 (m) $\frac{1}{2}$ CH2-C6, 3.83 (ddd) H5, 5.23 (d) H1	L, K, D, J, I, C
23	β-Glucose	3.24 (dd) H2, 3.40 (t) H4, 3.47 (ddd) H5, 3.48 (t) H3, 3.84 (m) $\frac{1}{2}$ CH_2-C6, 3.90 (dd) $\frac{1}{2}$ CH_2-C6, 4.64 (d) H1	L
24	Glutamate	2.08 (m) βCH_2, 2.34 (m) γCH_2, 3.75 (m) αCH	K, D, J, I, C
25	Glutamine	2.15 (m) βCH_2, 2.46 (m) γCH_2, 3.77 (m) αCH	L, K, D, J, I, C
26	Glutathione (oxidized)	2.17 (m) βCH_2 Glu, 2.55 (m) γCH_2 Glu, 2.98 (AB of ABX, broad) and 3.30 (AB of ABX, broad) βCH_2 Cys, 3.78, αCH_2 Gly, 4.75 (X of ABX, broad) αCH Cys	L
27	Glycine	3.56 (s) αCH	U, D, J, I
28	Glycerophosphocholine	3.23 (s) N-$(CH_3)_3$, 4.32 (m broad) CH	D, J, C
29	Glycogen	3.83 (m broad), 5.41 (m broad)	L
30	Guanine	7.72 (s) CH	U
31	Guanosine	3.86 (m) CH_2, 4.24 (m) H5, 4.41 (t) H4′, 5.91 (d) H2′, 8.00 (s) H8	U, D, J
32	Hippurate	3.97 (d) CH_2, 7.56 (t) m-CH, 7.65 (t) p-CH, 7.84 (d) αCH	U
33	Histidine	3.14 $\frac{1}{2}$ βCH_2 (AB of ABX), 3.25 $\frac{1}{2}$ βCH_2 (AB of ABX), 3.99 αCH (X of ABX), 7.08 (s) H5, 7.83 (s) H3	L, K
34	Hypotaurine	2.64 (t) CH_2-NH_2, 3.37 (t) CH_2-SO_3	L
35	Inosine	3.85 $\frac{1}{2}$ CH_2 (AB of ABX), 3.92 $\frac{1}{2}$ CH_2 (AB of ABX), 4.28 H5′ (X of ABX), 6.10 (d) H2′, 8.24 (s) H8, 8.34 (s) H2	L, K, D, J, I, C
36	Isoleucine	0.95 (t) δCH_3, 1.01 (d) βCH_3, 1.26 (m) $\frac{1}{2}$ γCH_2, 1.48 (m) $\frac{1}{2}$ γCH_2, 1.98 (m) βCH 3.68 (d) αCH	U, L, K, D, J, I, C
37	Isovaleric acid	0.92 (d) CH_3, 1.94 (m) CH, 2.05 (d) CH_2	U
38	Lactate	1.33 (d) βCH_3, 4.12 (q) αCH	L, K, D, J, I, C
39	Leucine	0.96 (d) δCH_3, 1.71 (m) γCH, 3.73 (t) αCH	L, K, D, J, I, C
40	Lysine	1.48 (m) γCH_2, 1.73 (m) δCH_2, 1.91 (m) βCH_2, 3.03 (t) εCH_2, 3.76 (t) αCH	K, D, J, I, C
41	*myo*-Inositol	3.29 (t) H5, 3.53 (dd) H1/H3, 3.63 (t) H4/H6, 4.06 (t) H2	K, D, J, C
42	*N*-Acetylcysteine	2.08 (s) CH_3, 2.94 (m) CH_2, 4.39 (m) CH	U
43	Nicotinurate	3.99 (s) CH_2, 7.6 (dd) H5, 8.25 (d) H4, 8.71 (d) H6, 8.94 (s) H2	L, K
44	Phosphocholine	3.22 (s) N-$(CH_3)_3$, 3.62 (t) βCH_2, 4.23 (m) αCH_2	L, I, C
45	Phenylacetylglycine	3.67 (s) δCH_2, 3.75 (d) αCH_2, 7.35 (m) H2/H6, 7.37 (t) H4, 7.42 (m) H3/H5	U
46	Phenylalanine	3.13 $\frac{1}{2}$ βCH_2 (AB of ABX), 3.28 $\frac{1}{2}$ βCH_2 (AB of ABX), 4.00 αCH (X of ABX), 7.33 (m) H2/H6, 7.39 (t) H4, 7.43 (m) H3/H5	L, K, D, J, I, C
47	Putrescine	1.80 (m broad) βCH_2, 3.05 (m broad) αCH_2	U
48	Raffinose	3.53 (s), 3.55–3.59 (m), 3.68 (s), 3.70–3.92 (m), 3.96 (t), 4.00–4.07 (m), 4.23 (d) H3 (fructose), 5.00 (d) H21 (galactose), 5.43 (d) H7 (glucose)	C
49	*scyllo*-Inositol	3.35 (s) CH	C
50	Succinate	2.41 (s) CH_3	U, L, K
51	Taurine	3.27 (t) CH_2-SO_3, 3.43 (t) CH_2-NH	U, L, K, D, J, I, C
52	Trimethylamine	2.86 (s) CH_3	U
53	Trimethylamine N-oxide	3.27 (s) $(CH_3)_3$	U, L
54	Tyrosine	3.06 $\frac{1}{2}$ βCH_2 (AB of ABX), 3.16 $\frac{1}{2}$ βCH_2 (AB of ABX), 3.94 αCH (X of ABX), 6.87 (d) H2/H6, 7.18 (d) H3/H5	L, K, D, J, I, C
55	Uridine diphosphate	4.21 (dd) $\frac{1}{2}$ CH_2, 4.25 (dd) $\frac{1}{2}$ CH_2, 4.37 (dt) H5, 4.39 (dd) H4, 4.43 H3, 5.96 (m) H2, 5.98 (d) H10, 7.98 (d) H11	U, L
56	Uracil	5.78 (d) CH, 7.52 (d) CH	I, C
57	Uridine	3.81 (dd) $\frac{1}{2}$ CH_2, 3.92 (dd) $\frac{1}{2}$ CH_2, 4.12 (dt) H5, 4.24 (dd) H4, 4.36 (dd) H3, 5.88 (d) H10, 5.92 (m) H2, 7.88 (d) H11	L, K, D, J
58	Uridine triphosphate	4.25 (dd) $\frac{1}{2}$ CH_2, 4.28 (dd) $\frac{1}{2}$ CH_2, 4.39 (dt) H5, 4.40 (dd) H4, 4.45(dd) H3, 5.90 (d) H10, 5.98 (m) H2, 7.98 (d) H11	L
59	Valine	0.99 (d) γCH_3, 1.05 (d) $\gamma' CH_3$, 2.28 (m) βCH, 3.62 (d) αCH	L, K, D, J, I, C

The numbering/nomenclature of compounds follows the IUPAC system.
Key: s, singlet; d, doublet, dd, doublet of doublets; t, triplet; m, multiplet; ABX refers to second-order spin system usually of the form CH_2CH where all three protons are non-equivalent; C, colon; D, duodenum; I, ileum; J, jejunum; K, kidney; L, liver; U, urine.

elimination of ammonia produced endogenously from the catabolism of amino acids, and exogenously from the degradation of proteins by gut microflora (Metzler, 2003) (Figure 7). The massive production of exogenous ammonium in colon lumen results in a high intake of ammonium in colonocytes where it is partially detoxified into urea (Mouillé *et al*, 1999). Thus, it is assumed that the observed lower levels of fumarate, glutamate, aspartate, alanine and lactate in GF profiles reflect the lower input of ammonia and/or the lower smooth muscle activity in these animals. All of these perturbations emphasize the fundamental role of gut microbiota in colonic epithelial metabolism.

Moreover, the liver metabotype of GF animals indicated other bacterial-related changes. A lower level of GSSG, the oxidized form of the powerful antioxidative compound GSH (Meister and Anderson, 1983) and a higher level of hypotaurine were observed in two GF animals of a total of four (Figure 2C). Despite the restricted numbers of individuals included in this study, it is possible that a subgroup of animals may exist. GSSG represents 1% of the total amount of glutathione *in vivo* (Deneke and Fanburg, 1989). In this study, GSH was not observed because it is readily oxidized to GSSG by exposure to atmospheric oxygen during sample preparation. Thus, it can be considered that the observed GSSG reflects the whole amount of glutathione in the liver extract. Normally, glutathione, rather than hypotaurine, is the predominant antioxidative molecule in the liver. Furthermore, it has been demonstrated that hypotaurine is also a strong antioxidative compound (Aruoma *et al*, 1988; Yancey, 2005). The observation of a high level of hypotaurine concomitant with low level of glutathione indicates a perturbation of the cell response to oxidative stress. Thus, for these two individuals, the higher level of hypotaurine may compensate for the lack of glutathione in the liver. It is noteworthy that the low total glutathione content was associated in these two animals with high levels of glycine, which is an essential amino acid for glutathione biosynthesis (Meister and Tate, 1976). Taken together, these observations indicate a perturbed γ-glutamyl cycle activity in the liver of two GF mice and this may be suggestive of altered cysteine metabolism (Meister, 1988). The low level of total glutathione in GF animals may impact on many metabolic pathways as it is also a coenzyme involved in the regulation of protein synthesis and degradation, as well as

Table II Summaries of O-PLS-DA statistical models

Sample	Orthogonal component	Q^2Y	R^2X
Duodenum	0	0.57	0.27
Jejunum	1	0.37	0.52
Ileum	0	0.46	0.26
Colon	1	0.70	0.34
Liver	1	0.58	0.47
Kidney	1	0.42	0.61
Urine	1	0.83	0.39

Q^2Y, cross-validated predicted percentage of the response Y; R^2X, variation of X explained by the model.

Table III Summary of variations of metabolite signals with the highest discriminant power for each model

Metabolite	δ (p.p.m.)	Duodenum	Jejunum	Ileum	Colon	Liver	Kidney	Urine
3-HCA	7.07							−0.93
4-HPP	6.89							−0.92
5-Aminovalerate	2.236				−0.86			
Alanine	1.476	+0.84		−0.83				
Aspartate	2.81			−0.84				
Betaine	3.904						+0.98	
Choline	3.2052						+0.94	
Creatine	3.04		+0.52		−0.83			
Creatinine	4.08							+0.89
Ethanolamine	3.1448						+0.87	
Formate	8.459				−0.76			
Fumarate	6.520			−0.79	−0.91			
Glutamate	2.078			−0.85				
Glutathione	2.5528					−0.71		
Glycine	3.559		+0.49			+0.79		
GPC	3.2312	−0.85			−0.85			
Hippurate	7.84							−0.93
Hypotaurine	2.645					+0.60		
Inosine	8.3468						+0.88	
Lactate	1.336			−0.79	−0.78			
Nac	2.185							−0.76
myo-Inositol	3.5288				−0.76		+0.92	
PAG	7.38							−0.87
Phosphocholine	3.2252				−0.76	+0.93		
Raffinose	5.435				+0.86			
scyllo-Inositol	3.3485				−0.72		+0.78	
Tauro-conjugated bile acids	0.697	+0.93	+0.51	+0.78		+0.66		
TMAO	3.269					+0.85		
Tyrosine	6.909		−0.81					
Uracil	5.811				−0.94			

Full chemical shift data for each metabolite are reported in Table I. The correlation coefficients with the discriminant axis for the metabolites involved in the difference between GF and conventional animals are presented as either higher (+) or lower level (−) compared with the conventional control.

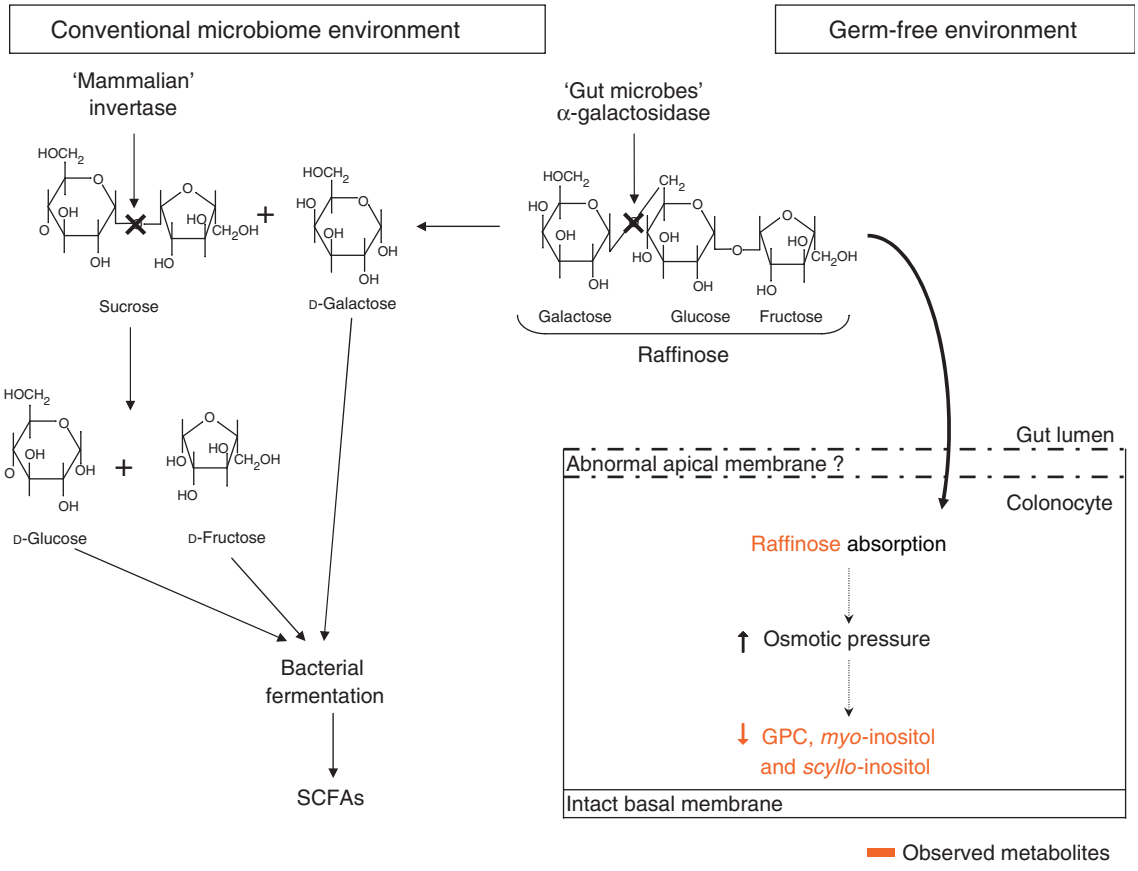

Figure 6 Variation of raffinose metabolism by colonocytes in germ-free (GF) and conventional microbiome animals. In conventional animals, raffinose is first digested by microbial α-galactosidase to release galactose and sucrose. Then, the mammalian invertase attached to the brush border releases glucose and fructose from sucrose. These monosaccharides are then utilized as a source of carbon for bacterial fermentation. In GF animals, raffinose is not catabolized and passive diffusion into colonocytes may occur contributing to the osmotic pressure that is regulated by decreasing levels of the mobile osmolytes: glycerophosphocholine, *myo*-inositol and *scyllo*-inositol. GPC, glycerophosphocholine; SCFAs, short chain fatty acids.

in the mechanism of immune system and in the prostaglandin metabolism (Meister and Anderson, 1983; DeLeve and Kaplowitz, 1991; Uhlig and Wendel, 1992; Wang and Ballatori, 1998).

TMAO variation contributes to the statistical separation between the metabolic profiles of livers from GF and conventional mice (Figure 2C). TMAO was expected to be lower in GF animals as previously observed in urine profiles during re-colonization of GF rats (Nicholls *et al*, 2003). Here, we observed a significantly higher level of TMAO in GF mice. TMAO in the liver derives either from a direct absorption of TMAO contained in the diet, from the gut microbial processing of choline and carnitine, or is endogenously synthesized by the oxidation of TMA to TMAO by the flavin-containing monooxygenase isomer 3 (FMO3) (Smith *et al*, 1994; Zhang *et al*, 2007). As the two groups were fed exactly the same diet, it can be deduced that the higher level of TMAO found in the liver of GF animals comes from either a greater uptake of TMA/TMAO contained in the diet, or from a higher endogenous synthesis. In contrast to humans, expression of FMO3 in mouse is sex dependent with a much lower expression in males. However, it has been recently demonstrated that this expression is highly inducible by TCDD (dioxin) in an aryl hydrocarbon receptor-dependent manner (Tijet *et al*, 2006). Thus, it is possible that FMO3 in male GF animals was induced.

A lower level of N-acetylated glycoprotein (Nac) signal was observed in the urine of GF animals (Figure 1C). This signal comes from the most abundant glycoprotein in urine, the Tamm–Horsfall protein (THP), also known as uromodulin, a small glycoprotein (~90 kDa) secreted by the thick ascending limb of the Henle's loop of the nephron (Serafini-Cessi *et al*, 2003). This protein is of particular interest in that its role is associated with the prevention of urinary tract infections. The N-glycans at the protein surface bind to uropathogenic strains of *Escherichia coli*, preventing the adhesion of these pathogens to the bladder wall (Pak *et al*, 2001; Mo *et al*, 2004). Here, the observed lower levels of Nac in GF urine profiles may be caused by a lower amount of THP in the urine or by a lower glycosylation of the protein. The protective function of THP is driven by N-glycans, so this observation reveals that protection against urinary tract pathogens is affected in the absence of gut microbiota. Also, choline, betaine, *myo*-inositol and *scyllo*-inositol were elevated in kidneys from GF mice (Figure 3C). All these metabolites are osmoprotectants (Burg, 1995) and it has been shown that their level increases in kidney cells when the environment becomes hypertonic

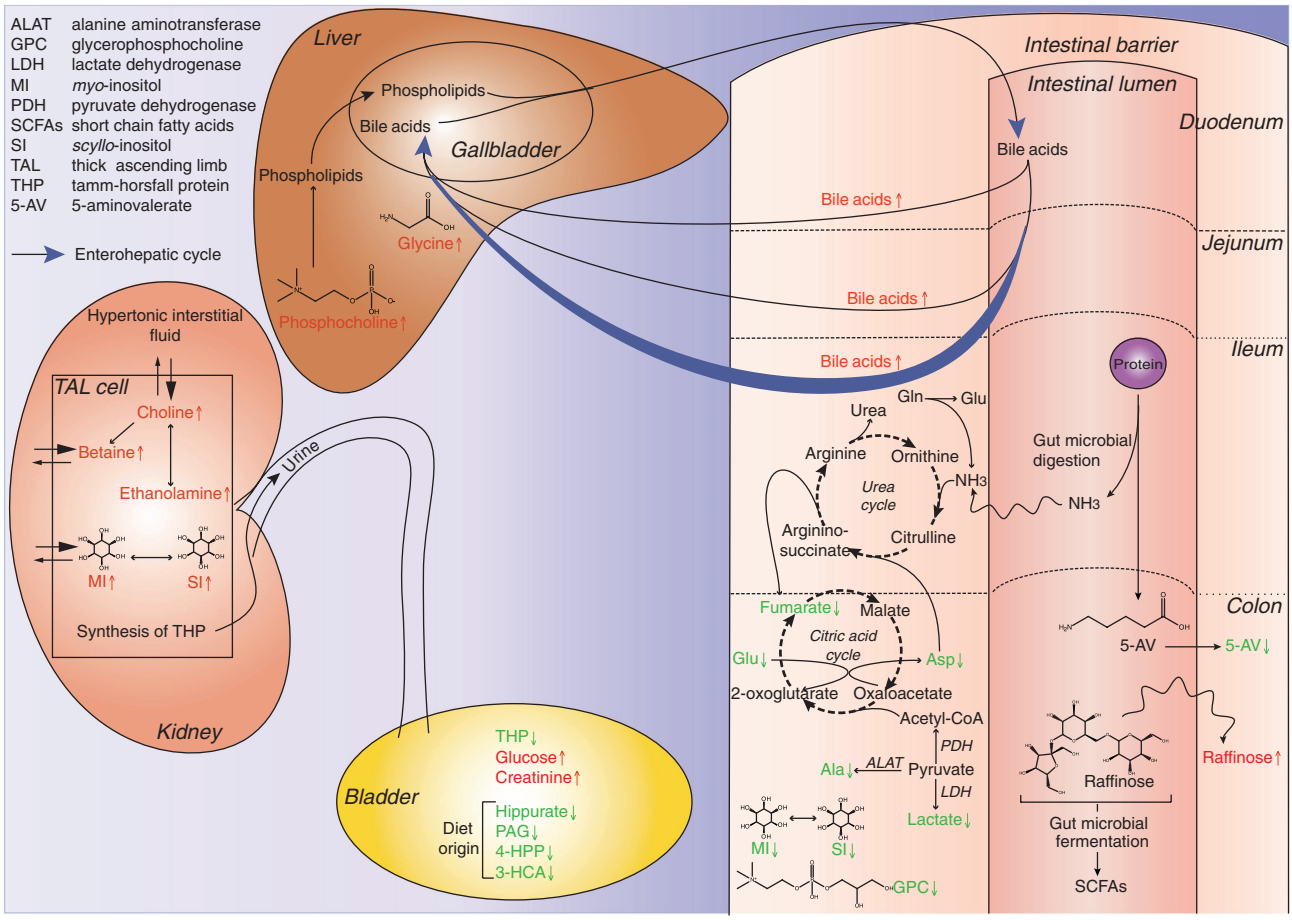

Figure 7 Summary of some of the major systemic effects of the gut microbiome on mouse metabolism in different compartments. Metabolites observed in this study are shown in red when their level is higher in GF profiles or in green when it is lower. The enterohepatic cycle of bile acids is shown as blue arrows. The citric acid cycle has been simplified for clarity.

(Yamauchi *et al*, 1991; Burg, 1995; Beck *et al*, 1998; Burger-Kentischer *et al*, 1999). Both decrease in THP concentration in urine and hypertonicity of interstitial fluid in kidney have been associated with renal dysfunction (Seldin and Giebisch, 2000), but it was not possible in this study to establish a link between these two observations.

Finally, the observed increased excretion of creatinine, a biomarker of muscle mass, in the urine of GF mice (Figure 1) is likely related to the lean phenotype of GF mice, as confirmed in a recent study (Bäckhed *et al*, 2007). Collectively, these data demonstrate that gut microbiota have a function in the control of the metabolic phenotype of the colon and liver and influence the whole-body metabolic homeostasis of the host.

Conclusions

We have demonstrated that gut microbiotal activities have an impact on site-specific intestinal epithelial biochemistry and influence at 'long-range' hepatic and renal metabolite profiles as well as the global metabolic phenotype of the host (summarized in Figure 7). It would be of considerable interest to correlate the compartmentalized metabolite profiles with the known bacterial strains that compose the microbiota and this is the focus of an ongoing investigation. Gut microbiota seem to be an important regulator of the bile acid metabolism and may have an impact on CYP enzyme induction status. These results also suggest the potential impact of the gut microbiota on antioxidant mechanisms in the liver but further studies are needed. We also show that gut microbiome influences the renal metabolite profile possibly in response to interstitial hypertonicity. By acting directly or indirectly on the metabolism of liver and kidney, key organs of body physiology (i.e. homeostasis of arterial pressure and equilibrium of cholesterol and electrolyte levels), the gut microbiota can be considered as a major contributor of host homeostasis. Improved knowledge of host–microbiome interactions will lead to a better understanding of individual variation in relation to health status and interventional outcomes (Clayton *et al*, 2006; Nicholson, 2006).

Materials and methods

Animal handling and sample preparation

All studies were conducted according to the Swiss legislation on animal experimentation.

One group of five GF C3H/HeJ mice (Charles River, France) was maintained in isolators on γ-ray-irradiated food (R03-10) and γ-ray-

irradiated water, whereas the other group of five conventional C3H/HeJ mice was maintained under identical conditions but in a conventional environment with non-irradiated food and water. Isolators were checked every week for any bacterial contamination throughout the life of GF animals. Throughout the duration of the study, water and food were provided *ad libitum*. Mice were euthanized when they were 8 weeks old, at which time urine and organs (duodenum, jejunum, ileum, colon, liver and kidney) were collected. Samples were snap frozen in liquid nitrogen and stored at −80°C until analysis.

^{1}H NMR spectroscopy

Urine samples were freeze-dried and dissolved in 50 μL of phosphate buffer 0.2 M (pH 7.4) in D_2O plus 0.05% sodium 3-(tri-methylsilyl)-propionate-2,3-d4 (TSP) before transferring to capillary tubes for analysis by ^{1}H NMR spectroscopy.

Tissue samples were homogenized and extracted in acetonitrile/water (1:1), as previously described (Waters *et al*, 2002). The supernatant containing the aqueous phase was collected, freeze-dried and dissolved in 600 μl of D_2O. Samples were centrifuged for 10 min at 15 000 *g*, and 500 μl of the supernatant and 50 μl of water were used for later analysis by NMR spectroscopy.

All ^{1}H NMR spectra were acquired on a Bruker Avance 600 MHz Spectrometer (Bruker Analytische GmbH, Rheinstetten, Germany) operating at 600.13 MHz and using a standard 1D pulse sequence (Nicholson *et al*, 1995) (recycle delay (RD)–90°–t_1–90°–t_m–90°–acquire free induction decay (FID)) with water suppression applied during RD of 2 s and mixing time (t_m) of 100 ms and a 90° pulse set at 9.75 μs. Spectra were acquired using 256 scans into 32K data points with a spectral width of 12 000 Hz. The FIDs were multiplied by an exponential function corresponding to 0.3 Hz line broadening. Zero filling of a factor of four for all tissue extracts and two for urine samples was also applied to the FIDs. All spectra were manually phased, baseline corrected and calibrated to lactate (δ 1.33) for tissue extracts and to TSP (δ 0.00) for urine samples. Metabolites were assigned using data from literature (Nicholson *et al*, 1995; Fan, 1996; Garrod *et al*, 2001) and additional two-dimensional (2D) NMR experiments on selected samples.

The 2D ^{1}H–^{1}H NMR spectra were performed on a Bruker DRX 400 Spectrometer operating at 400.13 MHz (Bruker Analytische GmbH) using 2D correlation spectroscopy (Aue *et al*, 1975) and total correlation spectroscopy (Glaser *et al*, 1996) experiments. 2D ^{1}H–^{13}C heteronuclear single quantum coherence NMR (Bodenhausen and Ruben, 1980) was performed on liver aqueous extracts on a Bruker DRX 500 Spectrometer operating at 499.9 MHz (Bruker Analytische GmbH) equipped with a 5 mm ^{1}H–^{13}C inverse cryoprobe.

Data analysis

To eliminate the variability in water resonance presaturation, the chemical shift region between δ 4.66 and 4.88 was removed from all spectra before statistical analysis, except for liver where to avoid bias due to baseline distortion, the region between δ 4.77 and 5.38 was removed. As previously described (Cloarec *et al*, 2005), all data were analyzed on full-resolution spectra (35 600 data points for liver and 36 500 data points for all other tissue extracts), normalized to the total peak area and models were constructed using O-PLS-DA with unit variance scaling on Matlab 7.0.1 software (The MathWorks Inc.). Despite the use of phosphate buffer, many urine spectra still displayed subtle pH-dependent shifts; therefore, the O-PLS-DA was performed on larger bins of 0.005 p.p.m. (1750 bucketed points) to minimize minor frequency changes in spatial components.

To aid interpretation, the O-PLS coefficients were plotted into a spectral domain using the back-scaling method (Cloarec *et al*, 2005). Using this method, the weights of each variable are back-scaled to their initial metric of the data and then the shape of NMR spectra and the sign of the coefficients are preserved. However, the weights of the variables can still be compared using a colour code corresponding to the square of the actual O-PLS coefficients. By construction, the O-PLS coefficients are directly proportional to the correlation coefficients between the discriminant axis and the NMR data. For this reason, the square of the coefficients can be represented in terms of correlation after applying the same corrective factor to all coefficients, allowing by this way an estimation of the amount of variance of each NMR variable involved in the discrimination.

Supplementary information

Supplementary information is available at the *Molecular Systems Biology* website (www.nature.com/msb).

Acknowledgements

This study was funded by Nestlé.

References

Albrecht J, Jones EA (1999) Hepatic encephalopathy: molecular mechanisms underlying the clinical syndrome. *J Neurol Sci* **170:** 138–146

Alfieri R (2007) Hyperosmotic stress response: comparison with other cellular stresses. *Pflugers Arch* **454:** 173–185

Alvaro D, Cantafora A, Attili AF, Ginanni Corradini S, De Luca C, Minervini G, Di Biase A, Angelico M (1986) Relationships between bile salts hydrophilicity and phospholipid composition in bile of various animal species. *Comp Biochem Physiol B* **83:** 551–554

Amieva MR, El-Omar EM (2008) Host–bacterial interactions in *Helicobacter pylori* infection. *Gastroenterology* **134:** 306–323

Aruoma OI, Halliwell B, Hoey BM, Butler J (1988) The antioxidant action of taurine, hypotaurine and their metabolic precursors. *Biochem J* **256:** 251–255

Atkinson C, Frankenfeld CL, Lampe JW (2005) Gut bacterial metabolism of the soy isoflavone daidzein: exploring the relevance to human health. *Exp Biol Med (Maywood)* **230:** 155–170

Aue WP, Baartholdi E, Ernst RR (1975) Two-dimensional spectroscopy. Application to nuclear magnetic resonance. *J Chem Phys* **64:** 2229–2246

Bäckhed F, Ding H, Wang T, Hooper LV, Young Koh G, Nagys A, Semenkovich CF, Gordon JI (2004) The gut microbiota as an environmental factor that regulates fat storage. *Proc Natl Acad Sci USA* **102:** 11070–11075

Bäckhed F, Ley RE, Sonnenburg JL, Peterson DA, Gordon JI (2005) Host–bacterial mutualism in the human intestine. *Science* **307:** 1915–1920

Bäckhed F, Manchester JK, Semenkovich CF, Gordon JI (2007) Mechanisms underlying the resistance to diet-induced obesity in germ-free mice. *Proc Natl Acad Sci USA* **104:** 979–984

Barker HA (1981) Amino acid degradation by anaerobic bacteria. *Annu Rev Biochem* **50:** 23–40

Barker HA, D'Ari L, Kahn J (1987) Enzymatic reactions in the degradation of 5-aminovalerate by *Clostridium aminovalericum*. *J Biol Chem* **262:** 8994–9003

Bates JM, Mittge E, Kuhlman J, Baden KN, Cheesman SE, Guillemin K (2006) Distinct signals from the microbiota promote different aspects of zebrafish gut differentiation. *Dev Biol* **297:** 374–386

Beck F-X, Burger-Kentischer A, Müller E (1998) Cellular response to osmotic stress in the renal medulla. *Eur J Physiol* **436:** 814–827

Berg RD (1996) The indigenous gastrointestinal microflora. *Trends Microbiol* **4:** 430–435

Bodenhausen G, Ruben DJ (1980) Natural abundance ^{15}N NMR by enhanced heteronuclear spectroscopy. *Chem Phys Lett* **69:** 185–189

Bollard ME, Stanley EG, Lindon JC, Nicholson JK, Holmes E (2005) NMR-based metabonomic approaches for evaluating physiological influences on biofluid composition. *NMR Biomed* **18:** 143–162

Bourlioux P, Koletzko B, Guarner F, Braesco V (2003) The intestine and its microflora are partners for the protection of the host: report on the Danone Symposium 'The Intelligent Intestine', held in Paris, June 14, 2002. *Am J Clin Nutr* **78:** 675–683

Burg MB (1995) Molecular basis of osmotic regulation. *Am J Physiol* **268:** F983–F996

Burger-Kentischer A, Muller E, Marz J, Fraek ML, Thurau K, Beck FX (1999) Hypertonicity-induced accumulation of organic osmolytes in papillary interstitial cells. *Kidney Int* **55:** 1417–1425

Burkholder PR, McVeigh I (1942) Synthesis of vitamins by intestinal bacteria. *Proc Natl Acad Sci USA* **28:** 285–289

Claudel T, Staels B, Kuipers F (2005) The farnesoid X receptor—a molecular link between bile acid and lipid and glucose metabolism. *Artherioscler Thromb Vasc Biol* **25:** 2020–2031

Clayton TA, Lindon JC, Cloarec O, Antti H, Charuel C, Hanton G, Provost JP, Le Net JL, Baker D, Walley RJ, Everett JR, Nicholson JK (2006) Pharmaco-metabonomic phenotyping and personalized drug treatment. *Nature* **440:** 1073–1077

Cloarec O, Dumas M-E, Craig A, Barton RH, Lindon JC, Nicholson JK, Holmes E (2005) Evaluation of the O-PLS model limitations caused by chemical shift variability and improved visualization of biomarker changes in ^{1}H NMR spectroscopic metabonomic studies. *Anal Chem* **77:** 517–526

DeLeve LD, Kaplowitz N (1991) Glutathione metabolism and its role in hepatotoxicity. *Pharmacol Ther* **52:** 287–305

Deneke SM, Fanburg BL (1989) Regulation of cellular glutathione. *Am J Physiol* **257:** L163–L173

Dumas ME, Barton RH, Toye A, Cloarec O, Blancher C, Rothwell A, Fearnside J, Tatoud R, Blanc V, Lindon JC, Mitchell SC, Holmes E, McCarthy MI, Scott J, Gauguier D, Nicholson JK (2006a) Metabolic profiling reveals a contribution of gut microbiota to fatty liver phenotype in insulin-resistant mice. *Proc Natl Acad Sci USA* **103:** 12511–12516

Dumas ME, Maibaum EC, Teague C, Ueshima H, Zhou B, Lindon JC, Nicholson JK, Stamler J, Elliott P, Chan Q, Holmes E (2006b) Assessment of analytical reproducibility of ^{1}H NMR spectroscopy based metabonomics for large-scale epidemiological research: the INTERMAP Study. *Anal Chem* **78:** 2199–2208

Dunne C (2001) Adaptation of bacteria to the intestinal niche: probiotics and gut disorder. *Inflamm Bowel Dis* **7:** 136–145

Fan TWM (1996) Metabolite profiling by one- and two-dimensional NMR analysis of complex mixtures. *Prog Nucl Magn Reson Spectrosc* **28:** 161–219

Garrod S, Humpher E, Connor SC, Connelly JC, Spraul M, Nicholson JK, Holmes E (2001) High-resolution ^{1}H NMR and magic angle spinning NMR spectroscopic investigation of the biochemical effects of 2-bromoethanamine in intact renal and hepatic tissue. *Magn Reson Med* **45:** 781–790

Gavaghan CL, Holmes E, Lenz E, Wilson ID, Nicholson JK (2000) An NMR-based metabonomic approach to investigate the biochemical consequences of genetic strain differences: application to the C57BL10J and Alpk:ApfCD mouse. *FEBS Lett* **484:** 169–174

Glaser SJ, Schwalbe H, Marino JP, Griesinger C (1996) Direct TOCSY, a method for selection of directed correlations by optimal combinations of isotropic and longitudinal mixing. *J Magn Reson B* **112:** 160–180

Goodwin BL, Ruthven CR, Sandler M (1994) Gut flora and the origin of some urinary aromatic phenolic compounds. *Biochem Pharmacol* **47:** 2294–2297

Hofmann AF (1999) The continuing importance of bile acids in liver and intestinal disease. *Arch Intern Med* **159:** 2647–2658

Holmes E, Nicholson JK (2005) Variation in gut microbiota strongly influences individual rodent phenotypes. *Toxicol Sci* **87:** 1–2

Hooper LV, Gordon JI (2001) Commensal host–bacterial relationships in the gut. *Science* **292:** 1115–1118

Hooper LV, Midtvedt T, Gordon JI (2002) How host–microbial interactions shape the nutrient environment of the mammalian intestine. *Annu Rev Nutr* **22:** 283–307

Hosokawa T, Kikuchi Y, Nikoh N, Shimada M, Fukatsu T (2006) Strict host–symbiont cospeciation and reductive genome evolution in insect gut bacteria. *PLoS Biol* **4:** 1841–1851

Houten SM, Watanabe M, Auwerx J (2006) Endocrine functions of bile acids. *EMBO J* **25:** 1419–1425

Kawamata Y, Fujii R, Hosoya M, Harada M, Yoshida H, Miwa M, Fukusumi S, Habata Y, Itoh T, Shintani Y, Hinuma S (2003) A G protein-coupled receptor responsive to bile acids. *J Biol Chem* **278:** 9435–9440

Koga N, Inskeep PB, Harris TM, Guengerich FP (1986) *S*-[2-(N7-Guanyl)ethyl]glutathione, the major DNA adduct formed from 1,2-dibromoethane. *Biochemistry* **25:** 2192–2198

Kostenis E (2004) A glance at G-protein-coupled receptors for lipid mediators: a growing receptor family with remarkably diverse ligands. *Pharmacol Ther* **102:** 243–257

LeBlanc JG, Silvestroni A, Connes C, Juillard V, Savoy de Giori G, Piard JC, Sesma F (2004) Reduction of non-digestible oligosaccharides in soymilk: application of engineered lactic acid bacteria that produce α-galactosidase. *Genet Mol Res* **3:** 432–440

Ley RE, Turnbaugh PJ, Klein S, Gordon JI (2006) Microbial ecology: human gut microbes associated with obesity. *Nature* **444:** 1022–1023

Lien YH, Michaelis T, Moats RA, Ross BD (1994) *scyllo*-Inositol depletion in hepatic encephalopathy. *Life Sci* **54:** 1507–1512

Lindon JC, Holmes E, Bollard ME, Stanley EG, Nicholson JK (2004) Metabonomics technologies and their applications in physiological monitoring, drug safety assessment and disease diagnosis. *Biomarkers* **9:** 1–31

Makishima M, Okamoto AY, Repa JJ, Tu H, Learned RM, Luk A, Hull MV, Lustig KD, Mangelsdorf DJ, Shan B (1999) Identification of a nuclear receptor for bile acids. *Science* **284:** 1362–1365

Manach C, Scalbert A, Morand C, Remesy C, Jimenez L (2004) Polyphenols: food sources and bioavailability. *Am J Clin Nutr* **79:** 727–747

Martin FP, Dumas ME, Wang Y, Legido-Quigley C, Yap IK, Tang H, Zirah S, Murphy GM, Cloarec O, Lindon JC, Sprenger N, Fay LB, Kochhar S, van BP, Holmes E, Nicholson JK (2007a) A top–down systems biology view of microbiome–mammalian metabolic interactions in a mouse model. *Mol Syst Biol* **3:** 112

Martin FP, Verdu EF, Wang Y, Dumas ME, Yap IK, Cloarec O, Bergonzelli GE, Corthesy-Theulaz I, Kochhar S, Holmes E, Lindon JC, Collins SM, Nicholson JK (2006) Transgenomic metabolic interactions in a mouse disease model: interactions of *Trichinella spiralis* infection with dietary *Lactobacillus paracasei* supplementation. *J Proteome Res* **5:** 2185–2193

Martin FP, Wang Y, Dumas ME, Cloarec O, Holmes E, Kochhar S, Sprenger N, Nicholson JK (2007b) Biochemical characterization of gut compartments in a germ-free mouse model and effects of *Lactobacillus paracasei* in mono-associated mice using high-resolution magic angle spinning ^{1}H NMR spectroscopy. *J Proteom Res* **6:** 1471–1481

Meister A (1988) Glutathione metabolism and its selective modification. *J Biol Chem* **263:** 17205–17208

Meister A, Anderson ME (1983) Glutathione. *Annu Rev Biochem* **52:** 711–760

Meister A, Tate SS (1976) Glutathione and related gamma-glutamyl compounds: biosynthesis and utilization. *Annu Rev Biochem* **645:** 559–604

Metges CC (2000) Contribution of microbial amino acids to amino acid homeostasis of the host. *J Nutr* **130:** 1857S–11864

Metzler DE (2003) The metabolism of nitrogen and amino acids. In *Biochemistry: the Chemical Reactions of Living Cells*, Hayhurst J (ed), pp 1358–1419. USA: Elsevier Science

Mo L, Zhu XH, Huang HY, Shapiro E, Hasty DL, Wu XR (2004) Ablation of the Tamm–Horsfall protein gene increases susceptibility of mice to bladder colonization by type 1-fimbriated *Escherichia coli*. *Am J Physiol Renal Physiol* **286:** F795–F802

Modica S, Moschetta A (2006) Nuclear bile acid receptor FXR as pharmacological target: are we there yet? *FEBS Lett* **580:** 5492–5499

Moreno A, Arus C (1996) Quantitative and qualitative characterization of ^{1}H NMR spectra of colon tumors, normal mucosa and their perchloric acid extracts: decreased levels of *myo*-inositol in tumours can be detected in intact biopsies. *NMR Biomed* **9:** 33–45

Mouillé B, Morel E, Robert V, Guihot-Joubrel G, Blachier F (1999) Metabolic capacity for L-citrulline synthesis from ammonia in rat isolated colonocytes. *Biochim Biophys Acta* **1427:** 401–407

Nicholls AW, Mortishire-Smith RJ, Nicholson JK (2003) NMR spectroscopic-based metabonomic studies of urinary metabolite variation in acclimatizing germ-free rats. *Chem Res Toxicol* **16:** 1395–1404

Nicholson JK (2006) Global systems biology, personalized medicine and molecular epidemiology. *Mol Syst Biol* **2:** 52

Nicholson JK, Connelly J, Lindon JC, Holmes E (2002) Metabonomics: a platform for studying drug toxicity and gene function. *Nat Rev Drug Discov* **1:** 153–161

Nicholson JK, Foxall PJ, Spraul M, Farrant RD, Lindon JC (1995) 750 MHz ^{1}H and ^{1}H–^{13}C NMR spectroscopy of human blood plasma. *Anal Chem* **67:** 793–811

Nicholson JK, Holmes E, Wilson ID (2005) Gut microorganisms, mammalian metabolism and personalized health care. *Nat Rev Microbiol* **3:** 431–438

Pak J, Pu Y, Zhang ZT, Hasty DL, Wu XR (2001) Tamm–Horsfall protein binds to type 1 fimbriated *Escherichia coli* and prevents *E. coli* from binding to uroplakin Ia and Ib receptors. *J Biol Chem* **276:** 9924–9930

Rezzi S, Ramadan Z, Fay LB, Kochhar S (2007) Nutritional metabonomics: applications and perspectives. *J Proteome Res* **6:** 513–525

Robosky LC, Wells DF, Egnash LA, Manning ML, Reily MD, Robertson DG (2005) Metabonomic identification of two distinct phenotypes in Sprague–Dawley (Crl:CD(SD)) rats. *Toxicol Sci* **87:** 277–284

Rohde CM, Wells DF, Robosky LC, Manning ML, Clifford CB, Reily MD, Robertson DG (2007) Metabonomic evaluation of Schaedler altered microflora rats. *Chem Res Toxicol* **20:** 1388–1392

Russell DW (2003) The enzymes, regulation, and genetics of bile acid synthesis. *Annu Rev Biochem* **72:** 137–174

Savage DC (1986) Gastrointestinal microflora in mammalian nutrition. *Annu Rev Nutr* **6:** 155–178

Seldin DW, Giebisch G (2000) *The Kidney: Physiology and Pathology.* Philadelphia, USA: Lippincott Williams & Wilkins

Serafini-Cessi F, Malagolini N, Cavallone D (2003) Tamm–Horsfall glycoprotein: biology and clinical relevance. *Am J Kidney Dis* **42:** 658–676

Setchell KD (1998) Phytoestrogens: the biochemistry, physiology, and implications for human health of soy isoflavones. *Am J Clin Nutr* **68:** 1333S–1346S

Smith JL, Wishnok JS, Deen WM (1994) Metabolism and excretion of methylamines in rats. *Toxicol Appl Pharmacol* **125:** 296–308

Tijet N, Boutros PC, Moffat ID, Okey AB, Tuomisto J, Pohjanvirta R (2006) Aryl hydrocarbon receptor regulates distinct dioxin-dependent and dioxin-independent gene batteries. *Mol Pharmacol* **69:** 140–153

Tsang TM, Woodman B, Mcloughlin GA, Griffin JL, Tabrizi SJ, Bates GP, Holmes E (2006) Metabolic characterisation of the R6/2 transgenic mouse model of Huntington's disease by high-resolution MAS ^{1}H NMR spectroscopy. *J Proteome Res* **5:** 483–492

Turnbaugh PJ, Ley RE, Mahowald MA, Magrini V, Mardis ER, Gordon JI (2006) An obesity-associated gut microbiome with increased capacity for energy harvest. *Nature* **444:** 1027–1031

Uchida K, Nomura Y, Takeuchi N (1980) Effects of cholic acid, chenodeoxycholic acid, and their related bile acids on cholesterol, phospholipid, and bile acid levels in serum, liver, bile, and feces of rats. *J Biochem (Tokyo)* **87:** 187–194

Ueyama J, Nadai M, Kanazawa H, Iwase M, Nakayama H, Hashimoto K, Yokoi T, Baba K, Takagi K, Takagi K, Hasegawa T (2005) Endotoxin from various Gram-negative bacteria has differential effects on function of hepatic cytochrome *P*450 and drug transporters. *Eur J Pharmacol* **510:** 127–134

Uhlig S, Wendel A (1992) The physiological consequences of glutathione variations. *Life Sci* **51:** 1083–1094

Umesaki Y, Setoyama H (2000) Structure of the intestinal flora responsible for development of the gut immune system in a rodent model. *Microbes Infect* **2:** 1343–1351

Wang W, Ballatori N (1998) Endogenous glutathione conjugates occurrence and biological functions. *Pharmacol Rev* **50:** 335–356

Wang Y, Holmes E, Comelli EM, Fotopoulos G, Dorta G, Tang H, Rantalainen MJ, Lindon JC, Corthesy-Theulaz IE, Fay LB, Kochhar S, Nicholson JK (2007) Topographical variation in metabolic signatures of human gastrointestinal biopsies revealed by high-resolution magic-angle spinning ^{1}H NMR spectroscopy. *J Proteome Res* **6:** 3944–3951

Wang Y, Tang H, Holmes E, Lindon JC, Turini ME, Sprenger N, Bergonzelli G, Fay LB, Kochhar S, Nicholson JK (2005) Biochemical characterization of rat intestine development using high-resolution magic-angle-spinning ^{1}H NMR spectroscopy and multivariate data analysis. *J Proteome Res* **4:** 1324–1329

Waters NJ, Holmes E, Waterfield CJ, Farrant RD, Nicholson JK (2002) NMR and pattern recognition studies on liver extracts and intact livers from rats treated with α-naphthylisothiocyanate. *Biochem Pharmacol* **64:** 67–77

Wehner F (2003) Cell volume regulation: osmolytes, osmolyte transport, and signal transduction. *Rev Physiol Biochem Pharmacol* **148:** 1–80

Williams RE, Eyton-Jones HW, Farnworth MJ, Gallagher R, Provan WM (2002) Effect of intestinal microflora on the urinary metabolic profile of rats: a ^{1}H-nuclear magnetic resonance spectroscopy study. *Xenobiotica* **32:** 783–794

Williams RE, Lenz EM, Evans JA, Wilson ID, Granger JH, Plumb RS, Stumpf CL (2005) A combined ^{1}H NMR and HPLC-MS-based metabonomic study of urine from obese (fa/fa) Zucker and normal Wistar-derived rats. *J Pharm Biomed Anal* **38:** 465–471

Wostmann BS (1981) The germfree animal in nutritional studies. *Annu Rev Nutr* **1:** 257–279

Yamauchi A, Kwon HM, Uchida S, Preston AS, Handler JS (1991) *Myo*-inositol and betaine transporters regulated by tonicity are basolateral in MDCK cells. *Am J Physiol* **261:** F197–F202

Yancey PH (2005) Organic osmolytes as compatible, metabolic and counteracting cytoprotectants in high osmolarity and other stresses. *J Exp Biol* **208:** 2819–2830

Zhang J, Cerny MA, Lawson M, Mosadeghi R, Cashman JR (2007) Functional activity of the mouse flavin-containing monooxygenase forms 1, 3, and 5. *J Biochem Mol Toxicol* **21:** 206–215

